doi:10.1093/brain/awm303 *Brain* (2008), **131**, 447–459

Focal white matter changes in spasmodic dysphonia: a combined diffusion tensor imaging and neuropathological study

Kristina Simonyan,[1] Fernanda Tovar-Moll,[2] John Ostuni,[3] Mark Hallett,[4] Victor F. Kalasinsky,[5] Michael R. Lewin-Smith,[5] Elisabeth J. Rushing,[6] Alexander O. Vortmeyer[7] and Christy L. Ludlow[1]

[1]Laryngeal and Speech Section, Medical Neurology Branch, [2]Neuroimmunology Branch, [3]Clinicial Neurosciences Program, [4]Human Motor Control Section, Medical Neurology Branch, [5]Department of Environmental and Infectious Disease Sciences, [6]Department of Neuropathology and Ophthalmic Pathology, Armed Forces Institute of Pathology and [7]Surgical Neurology Branch, National Institute of Neurological Disorders and Stroke, National Institutes of Health

Correspondence to: Kristina Simonyan, MD, PhD, Laryngeal and Speech Section, Medical Neurology Branch, National Institute of Neurological Disorders and Stroke, National Institutes of Health, 10 Center Drive, Building 10, Room 5D38, Bethesda, MD 20892-1416, USA
E-mail: simonyak@ninds.nih.gov

Spasmodic dysphonia is a neurological disorder characterized by involuntary spasms in the laryngeal muscles during speech production. Although the clinical symptoms are well characterized, the pathophysiology of this voice disorder is unknown. We describe here, for the first time to our knowledge, disorder-specific brain abnormalities in these patients as determined by a combined approach of diffusion tensor imaging (DTI) and *postmortem* histopathology. We used DTI to identify brain changes and to target those brain regions for neuropathological examination. DTI showed right-sided decrease of fractional anisotropy in the genu of the internal capsule and bilateral increase of overall water diffusivity in the white matter along the corticobulbar/corticospinal tract in 20 spasmodic dysphonia patients compared to 20 healthy subjects. In addition, water diffusivity was bilaterally increased in the lentiform nucleus, ventral thalamus and cerebellar white and grey matter in the patients. These brain changes were substantiated with focal histopathological abnormalities presented as a loss of axonal density and myelin content in the right genu of the internal capsule and clusters of mineral depositions, containing calcium, phosphorus and iron, in the parenchyma and vessel walls of the posterior limb of the internal capsule, putamen, globus pallidus and cerebellum in the *postmortem* brain tissue from one patient compared to three controls. The specificity of these brain abnormalities is confirmed by their localization, limited only to the corticobulbar/corticospinal tract and its main input/output structures. We also found positive correlation between the diffusivity changes and clinical symptoms of spasmodic dysphonia ($r = 0.509$, $P = 0.037$). These brain abnormalities may alter the central control of voluntary voice production and, therefore, may underlie the pathophysiology of this disorder.

Keywords: laryngeal dystonia; corticobulbar tract; basal ganglia; neuroimaging; neuropathology

Abbreviations: ABSD = abductor spasmodic dysphonia; ADSD = adductor spasmodic dysphonia; CBT/CST = corticobulbar/corticospinal tract; CV = coefficient of variance; DTI = diffusion tensor imaging; FA = fractional anisotropy; HV = healthy volunteer; ROI = region of interest; SD = spasmodic dysphonia; SEM-EDXA = scanning electron microscopy with energy dispersive X-ray analysis; TBSS = tract-based spatial statistics

Received May 10, 2007. Revised November 20, 2007. Accepted November 22, 2007. Advance Access publication December 14, 2007

Introduction

Spasmodic dysphonia (SD) is a primary focal dystonia characterized by loss of voluntary control of vocal fold movements during speech production due to involuntary spasms in the laryngeal muscles. After onset in mid-life, symptoms progress gradually and remain chronic for life (Ludlow *et al.*, 1995). This disorder presents most often as the adductor type (ADSD) characterized by spasmodic bursts in the closing muscles of the vocal folds during vowel production, which result in voice breaks (Nash and

Ludlow, 1996). The less common abductor type (ABSD) exhibits slow vocal fold closure following voiceless consonants with intermittent breathy voice breaks (Edgar *et al.*, 2001). SD is a task-specific disorder, affecting voice only during speech, while emotional vocal expressions, such as laughter and cry, remain intact (Bloch *et al.*, 1985).

The pathophysiology of SD is poorly understood. Generally, the focal dystonias are assumed to involve basal ganglia dysfunction and disturbances in the sensory system that play an important role in development of motor control abnormalities (Berardelli *et al.*, 1998). Recent functional neuroimaging studies during voice and narrative speech production in ADSD found activation changes in the laryngeal/orofacial sensorimotor cortex and basal ganglia (Haslinger *et al.*, 2005; Ali *et al.*, 2006), which may contribute to the pathophysiology of SD. However, a fundamental question about the neurobiology of primary dystonia is whether an underlying pathology can be identified. Recently, *postmortem* abnormalities have been found in patients with Meige's syndrome (Kulisevsky *et al.*, 1988) and DYT1 dystonia (Zweig and Hedreen, 1988; McNaught *et al.*, 2004), but these were limited only to the brainstem. Surprisingly, no significant abnormalities have been found in the basal ganglia of these patients. Furthermore, neuropathology has never been reported in isolated focal dystonias, and, in particular, structural brain abnormalities in patients with spasmodic dysphonia have never been investigated.

Despite the paucity of neuropathological studies, an increasing number of neuroimaging studies have reported the presence of structural changes in patients with other forms of dystonia. Using DTI, reduced white matter integrity has been found in the subgyral region of the sensorimotor cortex in both manifesting and unaffected DYT1 carriers (Carbon *et al.*, 2004). In cervical dystonia, white matter changes have been identified in the genu and body of the corpus callosum as well as in the basal ganglia (Colosimo *et al.*, 2005). Another study in a group of patients with cervical dystonia, generalized dystonia and one patient with SD has found abnormalities in the white matter underlying the middle frontal and postcentral gyri and in the basal ganglia and thalamus with adjacent white matter (Bonilha *et al.*, 2007).

In this study, we aimed to examine the organization of white matter in SD using combined DTI and histopathological approaches. We hypothesized that these patients would have abnormalities in white matter tracts connecting the brain regions involved in voluntary voice production for speech. Task-specificity (Bloch *et al.*, 1985) suggests a separation of the affected voluntary voice production system, controlled by the laryngeal motor cortex, from the unaffected emotional voice production system, controlled by the anterior cingulate cortex (Jurgens, 2002). We hypothesized, therefore, that microstructural white matter changes in SD would be found only in the voluntary voice production system for speech, involving the corticobulbar pathway.

Material and Methods

DTI quantifies the random displacement of water molecules and provides an *in vivo* estimation of axonal organization in brain tissue (Basser *et al.*, 1994). DTI measures include anisotropy indices (e.g. fractional anisotropy, FA) to quantify the directionality of water diffusion and, therefore, reflect axonal integrity and tissue coherence. Diffusivity indices [e.g. Trace of diffusion tensor, Trace (*D*) and mean diffusivity, MD] quantify the magnitude of water movement independent of direction (Pierpaoli *et al.*, 1996). These measures are sensitive to *microstructural* brain tissue abnormalities not evident on conventional MRI (Pierpaoli *et al.*, 2001; Pfefferbaum and Sullivan, 2003).

Participants

Twenty patients with SD (14 ADSD, 6 ABSD; age 55.0 ± 10.0 years, mean ± standard deviation; 8 males/12 females) and 20 healthy volunteers (HV) (age 52.7 ± 9.5 years, mean ± standard deviation; 8 males/12 females) participated in the study. Physical examination was normal in all participants; none had a history of neurological disorders (other than SD in the patient group), psychiatric or otolaryngological problems. No other forms of primary or secondary dystonia were present in the patients or their immediate family members based on patients' medical histories.

The median duration of SD was 11.0 years (range from 1.5 to 27 years). All patients had failed to respond to voice and speech therapy; it was, however, unknown whether these patients' voice symptoms had worsened since onset. Sixteen patients had been on a regimen of botulinum toxin injections into their laryngeal muscles for several years to maintain their voice symptoms reduction. The median interval between the last botulinum toxin treatment and scanning session was 9 months (range from 3 to 42 months). Two ADSD and two ABSD patients had not previously been treated with botulinum toxin.

Video fiberoptic nasolaryngoscopy and speech testing confirmed diagnosis of SD as well as normal laryngeal function in HV. To assure that the patients had SD and not a functional or psychogenic voice disorder, all patients were required to have disorder-specific spasmodic voice breaks during conversational speech (Sapienza *et al.*, 2000; Barkmeier *et al.*, 2001; Edgar *et al.*, 2001). Diagnostic criteria included hyperadduction of the vocal folds during intermittent voice breaks on vowels for ADSD and prolonged vocal fold opening during breathy breaks on voiceless consonants for ABSD. None of the patients reported symptom-free periods after onset of SD or following voice therapy without regular botulinum toxin treatment. For the purposes of this study, patients agreed to forgo their usually scheduled botulinum toxin treatment in order to be symptomatic at the time of voice and speech testing and scanning. All participants provided written informed consent before taking part in the study, which was approved by the Institutional Review Board of the National Institute of Neurological Disorders and Stroke, National Institutes of Health.

Speech symptom recording and measurement

We quantified symptoms specific to SD that is voice breaks on vowels in ADSD patients and on prolonged voiceless consonants in ABSD patients (Barkmeier *et al.*, 2001; Edgar *et al.*, 2001). Before the scanning, voice and speech of 17 patients were recorded

digitally, while they repeated two sets of sentences: 10 sentences containing a high number of glottal stops before vowels to elicit symptoms of ADSD, and 10 sentences containing a high number of voiceless consonants (f/s/h/p/t/k) to elicit symptoms of ABSD. In all patients, digital speech recordings were made with a microphone positioned at a constant 2 inch mouth to microphone distance. The recorded samples were randomly ordered and anonymized before voice break counts were made by a speech-language pathologist with more than seven years of specialized experience with SD. The frequency of voice breaks in 20 sentences either on vowels or on voiceless consonants was counted (Bielamowicz and Ludlow, 2000; Barkmeier *et al.*, 2001); voice harshness in ADSD and breathiness in ABSD were rated using the Consensus Auditory-Perceptual Evaluation of Voice (CAPE-V) (Karnell *et al.*, 2007). Pearson correlation coefficients were computed to examine relationships between the speech symptoms and diffusion parameters ($P \leqslant 0.05$).

Data acquisition

Participants were scanned on a 3.0 Tesla GE Excite scanner using an eight-channel receive-only coil (General Electric Medical System, Milwaukee, WI, USA). A DTI sequence for whole brain coverage used a single-shot spin-echo echo-planar imaging sequence with paired gradient pulses positioned 180° around the refocusing pulse for diffusion weighting and sensitivity-encoding (ASSET) for rate 2 acceleration. Imaging parameters for the diffusion-weighted sequence were TE/TR = 73.4/13 000 ms, FOV = 2.4 × 2.4 cm^2; matrix = 96 × 96 mm^2 zero-filled to 256 × 256 mm^2; 54 contiguous axial slices with slice thickness of 2.4 mm. Diffusion was measured along 33 non-collinear directions with a b factor of 1000 s/mm^2. Three reference images were acquired with no diffusion gradients applied (b_0 scans). The same acquisition sequence was repeated two times.

For clinical evaluation, the T_2-weighted images were acquired (FSE-T2: TE/TR = 120/5100 ms; FOV = 2.4 × 2.4 cm^2; matrix = 256 × 256 mm; 54 axial slices with slice thickness of 2.4 mm; FLAIR: TE/TR = 12 000/102 ms; FOV = 2.4 × 2.4 cm^2; matrix = 160 × 160 mm; 28 slices with slice thickness of 5.0 mm).

Image post-processing

For each subject, DTI images were co-registered to correct for movement artifacts and eddy current distortion effects on EPI readout (Woods *et al.*, 1998; Jiang *et al.*, 2006). Raw diffusion-weighted images were visually inspected slice-by-slice for each subject, and distorted slices were excluded from analysis before tensor calculation. The diffusion tensor for each voxel was calculated based on the eigenvectors (v_1, v_2, v_3) and eigenvalues ($\lambda_1, \lambda_2, \lambda_3$) using multivariate fitting and diagonalization. After the FA and Trace (D) maps were calculated from the eigenvalues, colour-coded maps were generated from the FA values and the three vector elements of v_1 to visualize the white matter tract orientation (DtiStudio software) (Pajevic and Pierpaoli, 1999; Jiang *et al.*, 2006). The derived FA and Trace data were further analysed using two approaches: the unbiased whole-brain tract-based spatial statistics (TBSS) (Smith *et al.*, 2006) and *a priori* regions of interest (ROI) analyses.

To assess scanner inter-session variability, four HVs were re-scanned at least 2 weeks apart with the post-processing and calculation of the DTI-derived parameters repeated. Inter-session variability for FA and Trace was represented as percent coefficient of variance [CV = (standard deviation/mean) × 100].

Unbiased whole-brain analysis

To assess the global differences in the white matter fibre tracts between the SD and HV groups, whole-brain voxelwise statistical analyses of FA and Trace data were conducted using TBSS *without an a priori* assumption (FSL, FMRIB Software Library) (Smith *et al.*, 2006). Because two comparisons were being conducted, a criterion alpha of 0.025 ($P = 0.05/2$) was applied for analyses of both the FA and Trace datasets. FA and Trace images were first brain-extracted (Smith, 2002) and registered to a common space (MNI152) using constrained nonlinear registration (Image Registration Toolkit) (Rueckert *et al.*, 1999). The mean of all registered FA maps was generated and used to create a mean FA skeleton, which represented the centers of all tracts common to all subjects. Each subject's aligned FA and Trace data were registered to the common FA skeleton via a perpendicular search from each tract in the mean FA skeleton to each image's local tract center forming a sparse (skeletonized) 4D image. Statistical analyses for each point of the mean skeleton were conducted for both FA and Trace maps using univariate general linear modelling design (FEAT, FSL, FMRIB Software Library) to test for significant differences between the two groups. Correction for multiple comparisons was performed using permutation-based inference (5000 permutations) (Nichols and Holmes, 2002) with a cluster-forming threshold of $t > 3$ and a corrected cluster size significance level of $P \leqslant 0.025$ (randomize, FSL, FMRIB Software Library) (Smith *et al.*, 2006). This approach controlled for familywise errors (FWE) due to the chance of one or more false positives occurring anywhere on the skeleton while searching over the entire skeleton for regions of significant effect (Smith *et al.*, 2006).

ROI analysis

Because we hypothesized that regions involved in the control of voluntary voice production for speech, but not for emotional vocal expressions, would be affected in SD, we identified the two sets of ROIs for analysis. *A priori* ROIs were defined along the corticobulbar/corticospinal tract (CBT/CST) in the genu and the posterior third quarter of the posterior limb of the internal capsule, the mid-third of the cerebral peduncle and the pyramid. Furthermore, the ROIs were defined in the main input/output structures contributing to the CBT/CST: in the lentiform nucleus, the ventral thalamus and the middle third of the middle cerebellar peduncle. On the other hand, the ROIs in the cingulum underlying the anterior cingulate cortex were chosen to test the hypothesis that changes would not be present in the white matter tracts connecting the brain regions involved in the control of voice initiation and voice expression of emotional states (Jurgens, 2002), which remain unaffected in SD patients.

Prior to ROI analysis, the FA and Trace datasets were anonymized and randomized across the subjects and groups (J.O.). All ROIs were placed by the same rater (K.S.) blind to participants identity and diagnosis using a DTI-MRI atlas of human white matter (Mori, 2005) for determining fibre tract orientation. For each subject, the ROIs were outlined on the colour-coded FA maps in the axial plane as fixed-size squares to avoid arbitrary size of ROIs across participants (25 pixels/ROI along the CBT/CST; 36 pixel/ROI in the lentiform nucleus; 64 pixel/ROI in the thalamus) and then automatically loaded onto the FA and Trace

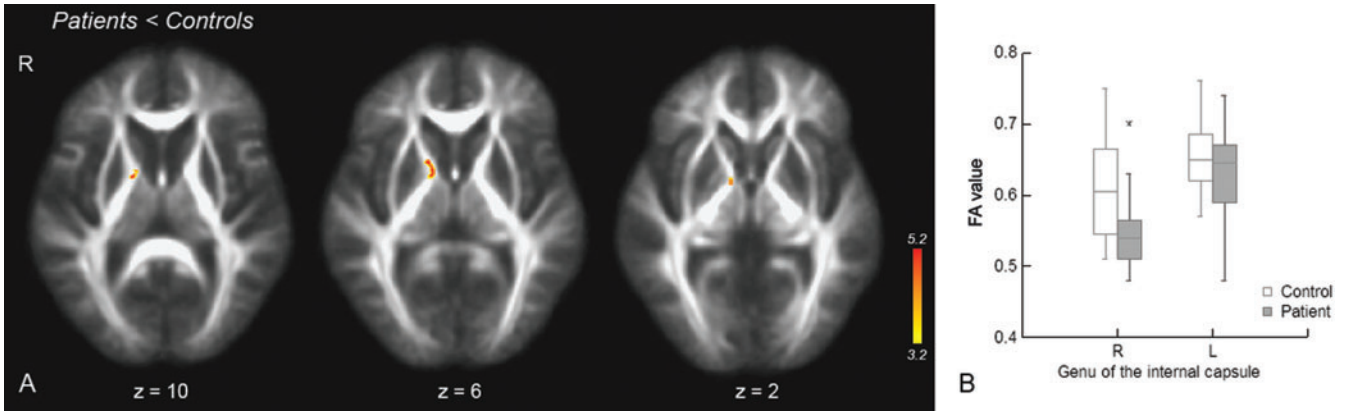

Fig. 1 Group differences in fractional anisotropy. (**A**) TBSS whole-brain and (**B**) a priori ROI analyses found significant FA decrease in the right genu of the internal capsule in SD patients. Group differences (patients < controls) are overlaid onto the average FA map across all subjects; plane coordinates of axial brain images are in Talairach-Tournoux standard space, respectively; colour bar indicates the significance range at $Z > 3.2$. Box plots indicate median and upper and lower quartiles. Error bars indicate the range between the 90th and 10th percentiles. Asterisk indicates significant difference between two groups. R = right; L = left.

maps (see supplementary Fig. 1 online). All ROIs were visually checked to confirm their location, to ensure that partial volume effects were minimized and that each ROI contained homogeneous fibre populations through examination of slices one dorsal and one caudal from the target. The mean values and standard deviations of FA and Trace measures within each ROI were automatically recorded.

To control for intra-observer variability, FA and Trace ROI values were re-calculated in six subjects at least 2 weeks apart to assess the percent coefficient of variance as a measure of repeatability.

Regression analyses examined age and gender effects on the FA and Trace values within each group to determine whether these factors needed to be used as covariates in group comparisons (Furutani *et al.*, 2005). Two-way repeated analyses of variance (ANOVA) were used for group (independent) comparisons, including all ROIs (repeated) on the right and left hemispheres (repeated) for both the FA and Trace values. The overall significance level was set at 0.025 ($P = 0.05/2$) for each of FA and Trace ANOVAs. If the group effects or their interactions on overall ANOVAs were statistically significant at $P \leqslant 0.025$, *post hoc* univariate *F*-tests determined which brain regions differed significantly between the groups. Because the Bonferroni correction for multiple comparisons for each of FA and Trace values resulted in an overly conservative correction ($P = 0.0016$) reducing power on the individual tests and increasing the possibility of a type II error, the statistical significance for post hoc tests was set at $P < 0.01$. The relationship between the FA and Trace values was assessed using Pearson's correlation coefficients at an alpha level of 0.05.

DTI-guided *postmortem* brain tissue sampling

To evaluate possible bases for DTI changes in SD, we targeted and sampled *postmortem* brain tissue in one SD patient and three controls from regions corresponding to FA and Trace changes between SD and HV groups. These matched *postmortem* tissue samples included regions of the right internal capsule, lentiform nucleus and cerebellum. *Postmortem* brain tissue from patient's left hemisphere as well as brain tissue from the regions of the sensorimotor cortex, corona radiata, thalamus and cerebral peduncle in the right hemisphere was not available to us for neuropathological examination. *Antemortem*, the patient (male, 65 years old) diagnosed with ADSD presented with strained voice quality and moderate adductor voice breaks during vowel production. The onset of the disorder was at age 36 years. The patient was diagnosed and treated at the National Institutes of Health with botulinum toxin injections into the thyroarytenoid muscles at regular intervals over 10 years. The brain tissue from this patient was obtained following death, which occurred during cardiac bypass surgery. The control brain tissue was obtained from three subjects (females; age range 58–86 years) without any history of neurological or psychiatric disorders, who died due to cardiovascular disease, disseminated intervascular coagulation, and dehydration with hypernatraemia, respectively.

The brain tissue from all subjects was fixed in 10% formalin solution and sectioned into 2-cm thick coronal slices for gross examination. Guided by the hardcopy of the T_1-weighted images in coronal plane with overlaid FA and Trace group differences, tissue samples were dissected from the right genu and posterior limb of the internal capsule, the lentiform nucleus and the cerebellum for paraffin embedding. For histopathological examination, paraffin sections (thickness 5 µm) were stained with hematoxylin and eosin (H&E) and luxol-fast blue/periodic acid Schiff (LFB/PAS) to assess cell morphology and myelin changes. The immunohistochemical markers, KP1 (anti-CD68) and anti-neurofilament triplet protein (anti-NFTP), were used for visualization of microglia/macrophage activation and the intermediate filament proteins of neuronal differentiation, respectively. In brief, sections were pre-treated with DAKO Target Retrieval Solution (DakoCytomation, Carpinteria, CA) at 95°C for 20 min, cooled at room temperature and incubated with primary antibody at dilution of 1 : 100 for 30 min (monoclonal mouse anti-human CD68, Clone KP1; monoclonal mouse anti-human neurofilament protein, Clone 2F11; DakoCytomation, Denmark). Primary antibodies were omitted for negative controls. The sections were then incubated with a refined avidin-biotin visualization kit (LSAB+ System-HRP, DakoCytomation, Carpinteria, CA) for 1 h.

For evaluation of Trace differences between SD and HV groups, subsequent sections from the internal capsule, lentiform nucleus and cerebellum were additionally processed with alizarin red S stain for visualization of calcium deposition, with von Kossa stain

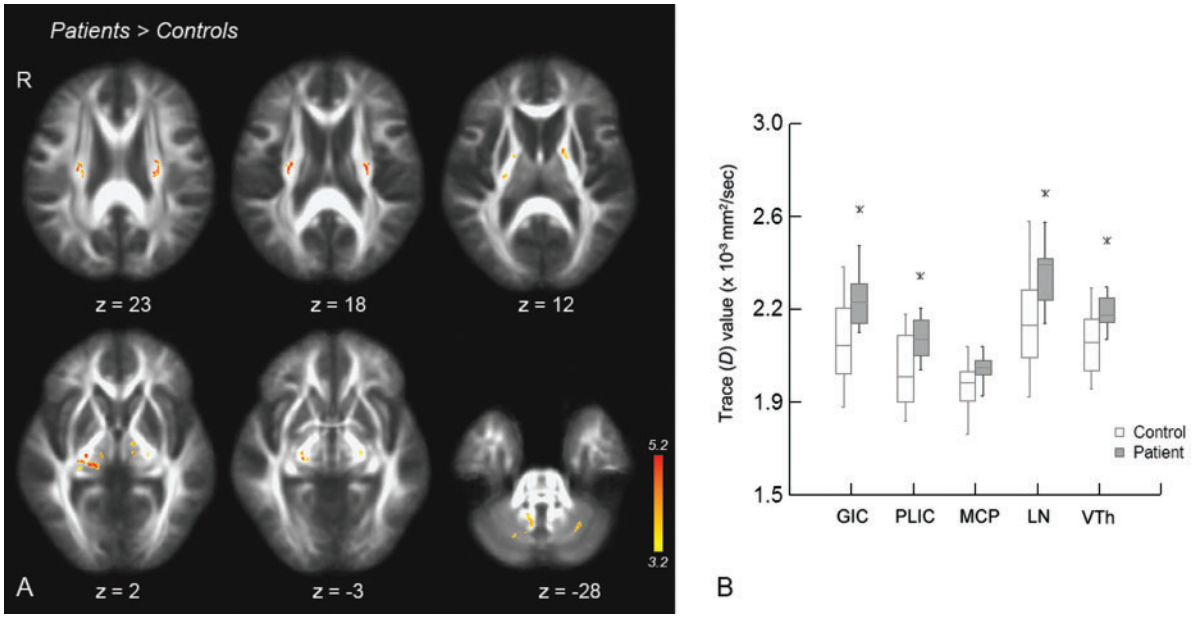

Fig. 2 Group differences in Trace (*D*). (**A**) TBSS whole-brain analysis found significant increase of overall diffusivity in the corona radiata, genu and posterior limb of the internal capsule, cerebral peduncle, ventral thalamus, and cerebellum. Group differences (patients > control) are overlaid onto the average FA map across all subjects; plane coordinates of axial brain images are in Talairach-Tournoux standard space, respectively; colour bar indicates the significance range at $Z > 3.2$. (**B**) *A priori* ROI analysis found significant increase of Trace values ($\times 10^{-3}$ mm^2/s) in the genu (GIC) and posterior limb (PLIC) of the internal capsule, lentiform nucleus (LN), and ventral thalamus (VTh) with a trend in the middle cerebellar peduncle (MCP) in SD patients. Box plots indicate median and upper and lower quartiles. Error bars indicate the range between the 90th and 10th percentiles. Asterisks indicate significant difference between two groups. R = right; L = left.

for phosphates and other anions, and with Prussian blue stain for iron accumulations, respectively. Furthermore, infrared spectroscopy was performed for routine molecular characterization of tissue depositions. Infrared spectra were obtained by focusing the infrared light onto tissue sections mounted on aluminium-coated glass slides (ThermoNicolet, Madison, WI). Spectra were recorded at 4 cm^{-1} spectral resolution. The measured infrared spectra were compared with those of the authentic samples and to spectra stored in a digital spectral library. To obtain the broader spectrum of elemental compositions of depositions found on H&E sections, a scanning electron microscope (Hitachi Instruments, Inc., San Jose, CA) with energy dispersive X-ray analysis (ThermoNoran, Madison, WI) (SEM-EDXA) was used to determine the particles with atomic numbers as low as that of beryllium. However, because of the difficulties in co-localization of the clusters on unstained section using SEM-EDXA, the analysis was limited to the parenchymal clusters located closely to the identifiable vessels in an unstained tissue sample. The EDXA detected the X-rays produced by the elements in the tissue samples when exposed to a 20 kV electron beam. X-rays were directed to the liquid-nitrogen-cooled silicon detector fitted with a Norvar® window.

Results

Conventional MRI was normal without any structural differences between patients and controls based on radiological evaluation. The inter-session variability results showed good reproducibility for both FA (CV of 4%) and Trace (CV of 2.1%). The intra-observer variability results also showed good reproducibility for both FA (CV of 2.30%) and Trace (CV of 0.53%). No significant relationships were found in either group between the diffusion parameters and age (FA: $r_{SD} = 0.088$, $P_{SD} = 0.713$; $r_{control} = 0.300$, $P_{control} = 0.199$; Trace: $r_{SD} = 0.141$, $P_{SD} = 0.552$; $r_{control} = 0.282$, $P_{control} = 0.228$) or gender (FA: $r_{SD} = 0.133$, $P_{SD} = 0.577$; $r_{control} = 0.084$, $P_{control} = 0.725$; Trace: $r_{SD} = 0.208$, $P_{SD} = 0.379$; $r_{control} = 0.137$, $P_{control} = 0.564$). Therefore, group comparisons were conducted without covariates.

Fractional anisotropy

The TBSS whole-brain analysis showed decreased FA only in the right genu of the internal capsule in SD patients compared with HV (Fig. 1A). The ANOVA comparison of ROI FA values did not demonstrate significant overall group differences ($F_{1,38} = 0.057$, $P = 0.812$), but determined significant ROI effect ($F_{7,266} = 584.525$, $P = 0.0005$) and group by ROI interaction ($F_{7,32} = 2.727$, $P = 0.024$) as well as a trend for a group by hemispheric laterality interaction ($F_{1,38} = 4.201$, $P = 0.047$). Significant regional differences between the two groups were again found in the right genu of the internal capsule ($F_{1,38} = 9.494$, $P = 0.004$) (Fig. 1B).

Trace (*D*) diffusivity

The TBSS whole-brain group comparison found increased Trace values in the corona radiata, the genu and posterior third quarter of the internal capsule, the middle third of cerebral peduncle, the cerebellar white and grey matter, and the ventral thalamus bilaterally in SD patients (Fig. 2A).

Table 1 DTI-derived measures in healthy controls and SD patients based on ROI analysis

Anatomical region		Fractional anisotropy		Trace (*D*) ($\times 10^{-3}$ mm^2/s)	
		Controls	Patients	Controls	Patients
Genu of internal capsule	R	0.61 ± 0.07	0.55 ± 0.05[a]	2.10 ± 0.20	2.22 ± 0.14[a]
	L	0.65 ± 0.05	0.63 ± 0.07	2.14 ± 0.17	2.34 ± 0.18[a]
Posterior limb of internal capsule	R	0.69 ± 0.05	0.70 ± 0.03	1.99 ± 0.15	2.11 ± 0.11[a]
	L	0.69 ± 0.04	0.70 ± 0.04	2.03 ± 0.15	2.12 ± 0.11[a]
Cerebral peduncle	R	0.74 ± 0.04	0.74 ± 0.05	2.14 ± 0.15	2.17 ± 0.14
	L	0.76 ± 0.05	0.76 ± 0.05	2.09 ± 0.17	2.17 ± 0.21
Pyramid	R	0.51 ± 0.08	0.52 ± 0.05	2.06 ± 0.18	2.15 ± 0.21
	L	0.51 ± 0.08	0.54 ± 0.07	2.09 ± 0.19	2.13 ± 0.14
Middle cerebellar peduncle	R	0.66 ± 0.05	0.66 ± 0.11	1.94 ± 0.11	2.04 ± 0.10
	L	0.62 ± 0.06	0.62 ± 0.08	1.94 ± 0.11	1.97 ± 0.08
Lentiform nucleus	R	0.19 ± 0.03	0.19 ± 0.07	2.11 ± 0.18	2.41 ± 0.21[a]
	L	0.15 ± 0.03	0.15 ± 0.04	2.17 ± 0.17	2.32 ± 0.11[a]
Ventral thalamus	R	0.28 ± 0.05	0.26 ± 0.03	2.04 ± 0.31	2.19 ± 0.19[a]
	L	0.31 ± 0.04	0.29 ± 0.05	2.10 ± 0.15	2.20 ± 0.27[a]
Cingulum	R	0.46 ± 0.09	0.49 ± 0.07	2.20 ± 0.30	2.26 ± 0.21
	L	0.52 ± 0.11	0.53 ± 0.08	2.30 ± 0.25	2.41 ± 0.21

Values report mean ± standard deviation. (a) indicates brain regions significantly different between patients and controls ($P \leqslant 0.01$). R = right, L = left.

The ANOVA overall group effect for the ROI analysis of Trace measures was significant ($F_{1,38} = 10.161$, $P = 0.003$) with non-significant group by ROI ($F_{7,32} = 1.433$, $P = 0.227$) or group by hemispheric laterality ($F_{1,38} = 1.812$, $P = 0.186$) interactions. Because of the lack of hemispheric differences, the right and left ROIs for Trace values were combined for univariate comparisons. Regional differences in Trace were found in the genu ($F_{1,38} = 10.601$, $P = 0.002$) and the posterior limb of the internal capsule ($F_{1,38} = 7.743$, $P = 0.008$), the lentiform nucleus ($F_{1,38} = 9.360$, $P = 0.004$) and the ventral thalamus ($F_{1,38} = 8.959$, $P = 0.005$). A group trend was found in the middle cerebellar peduncle ($F_{1,38} = 6.156$, $P = 0.018$) (Fig. 2B). Mean and standard deviation of FA and Trace values in SD patients and healthy controls are reported in Table 1.

Correlations between diffusion parameters and clinical scores

In all ROIs taken together, the mean FA and Trace values had significant inverse correlation, which was greater in SD patients ($r = -0.737$, $P = 0.0005$) than in HVs ($r = -0.465$, $P = 0.039$) (Fig. 3A). When the relationship between FA and Trace was examined in the regions that differed between the two groups, a significant inverse correlation was observed in the genu of the internal capsule in the patients ($r = -0.639$, $P = 0.002$), which was greater than the correlation in the HVs ($r = -0.454$, $P = 0.044$) (Fig. 3B).

The FA and Trace measures in the regions that differed between the two groups (FA in the right genu and Trace in the genu and posterior limb of the internal capsule, the lentiform nucleus and the ventral thalamus) were also examined for their relationships with numbers of voice breaks in sentences and duration of disorder in SD patients. We found positive correlation between the Trace values in the ventral thalamus and number of breaks during speech production ($r = 0.509$, $P = 0.037$) in SD patients (Fig. 3C).

Neuropathological evaluation

No gross abnormalities were found in either the patient or the control brains. Histopathological analysis of the genu of the right internal capsule revealed reduced white matter density due to moderate reduction of myelin content surrounded by scattered microglial/macrophage activation in the SD patient. Moderate focal reduction of axonal density was observed in the same locus in the SD patient (Fig. 4). No such changes were found in the tissue sampled from the anterior and posterior limbs of the internal capsule in either a patient or controls.

Neuropathological examination of the H&E sections, where Trace differences were found, identified clusters of dark-blue/black basophilic precipitates in the parenchyma and small-caliber vessels in the putamen, globus pallidus and the posterior limb of the internal capsule in the SD patient compared to controls (Fig. 5A–C). In the patient's cerebellum, small areas of basophilic deposits were distributed in the cortex and white matter. No axonal loss or demyelination was found in either of these brain regions. Histochemical stains of the brain sections from the putamen, globus pallidus and cerebellum with adjacent white matter demonstrated that the parenchymal clusters were selectively positive for calcium and phosphate with single scattered iron deposits. Depositions in the vessel wall were stronger positive for iron in addition to calcium and phosphorus (Fig. 5D and F). None of these changes was found in controls.

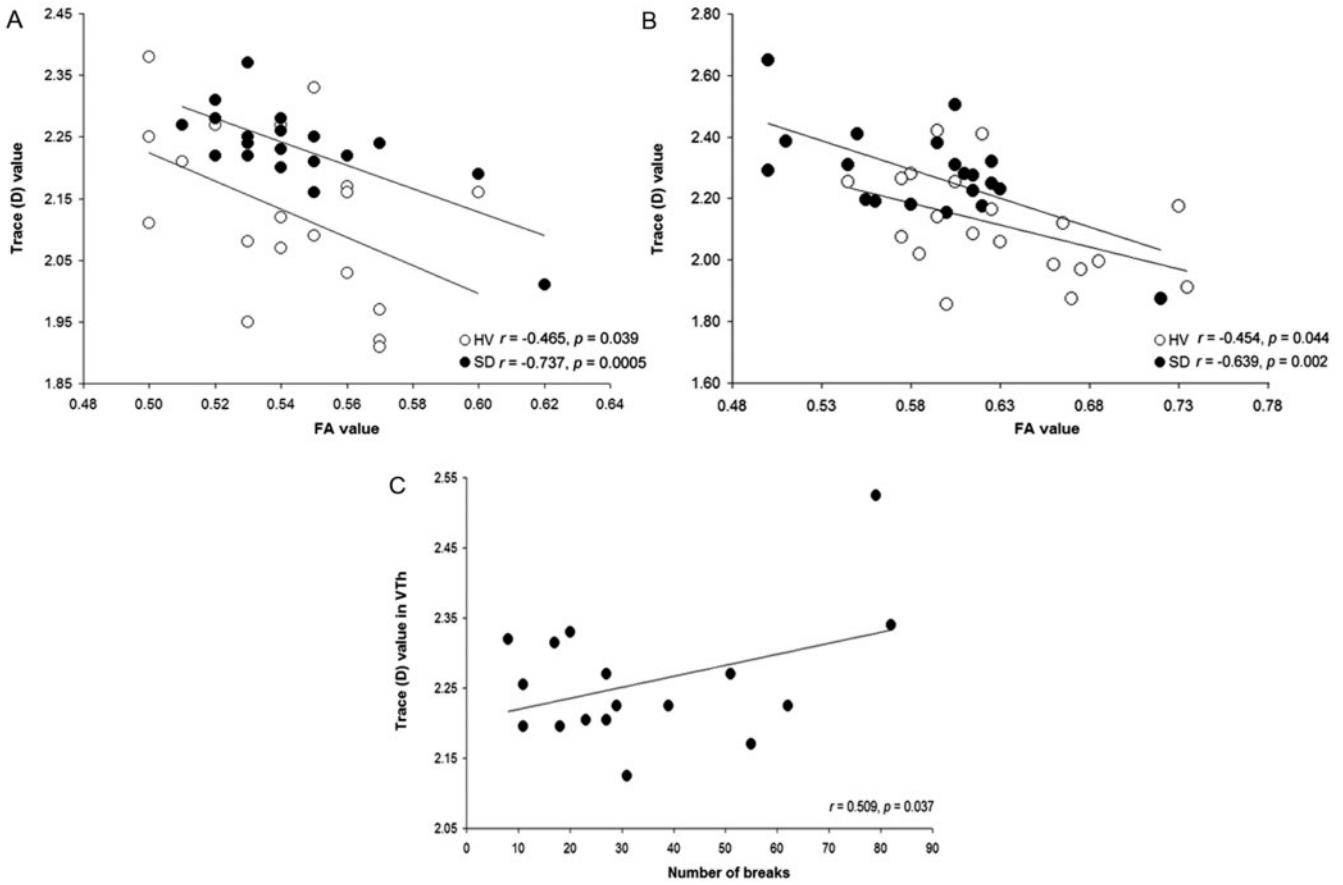

Fig. 3 Correlation between diffusion parameters. (**A**) Significant inverse correlation between overall mean values of fractional anisotropy (FA) and Trace (*D*) was stronger in SD patients than in HV. (**B**) Significant inverse correlation between the FA and Trace values were found in the genu of the internal capsule. (**C**) Positive significant correlation was determined between the Trace values in the ventral thalamus (VTh) and number of breaks in SD patients.

By infrared spectroscopy, spectra characteristic of phosphate were obtained from both the parenchymal and vessel wall deposits in the putamen, globus pallidus, internal capsule and cerebellum of the patient's tissue. The phosphate spectra most closely resembled the authentic infrared spectrum of apatite. SEM-EDXA of the representative deposition in the parenchyma demonstrated focal collocation of phosphorus and calcium in SD brain (Fig. 6A). This calcium phosphate was present admixed with protein, probably representing degenerated tissue protein. In the vessel wall, the SEM-EDXA map showed presence of iron in addition to calcium and phosphorus (Fig. 6B).

Discussion

In this study, we combined, for the first time to our knowledge, the neuroimaging and neuropathological approaches to examine the structural brain organization in patients with SD. Using DTI, we identified white matter changes along the CBT/CST and in the brain regions directly or indirectly contributing to this tract in SD patients. Consequently, we substantiated these findings with *postmortem* histopathological abnormalities presented as a focal reduction of axonal density and myelin content in the genu of the internal capsule and clusters of mineral accumulations in the parenchyma and vessel walls in the internal capsule, putamen, globus pallidus and cerebellum in SD. We also identified a significant statistical relationship between disorder symptom severity and the brain water diffusivity changes in SD. The brain abnormalities in SD found here could, therefore, be considered as primary brain changes contributing to the pathophysiology of this disorder.

Corticobulbar/corticospinal tract

Significant microstructural abnormalities were found in the CBT/CST in SD patients compared with controls. We suggest that SD may be associated with alterations in anatomical connectivity of the corticobulbar tract (CBT) descending from the laryngeal/orofacial motor cortex to the brainstem phonatory nuclei (Kuypers, 1958; Iwatsubo *et al.*, 1990). The CBT descends together with the CST via the corona radiata, internal capsule, cerebral peduncle and

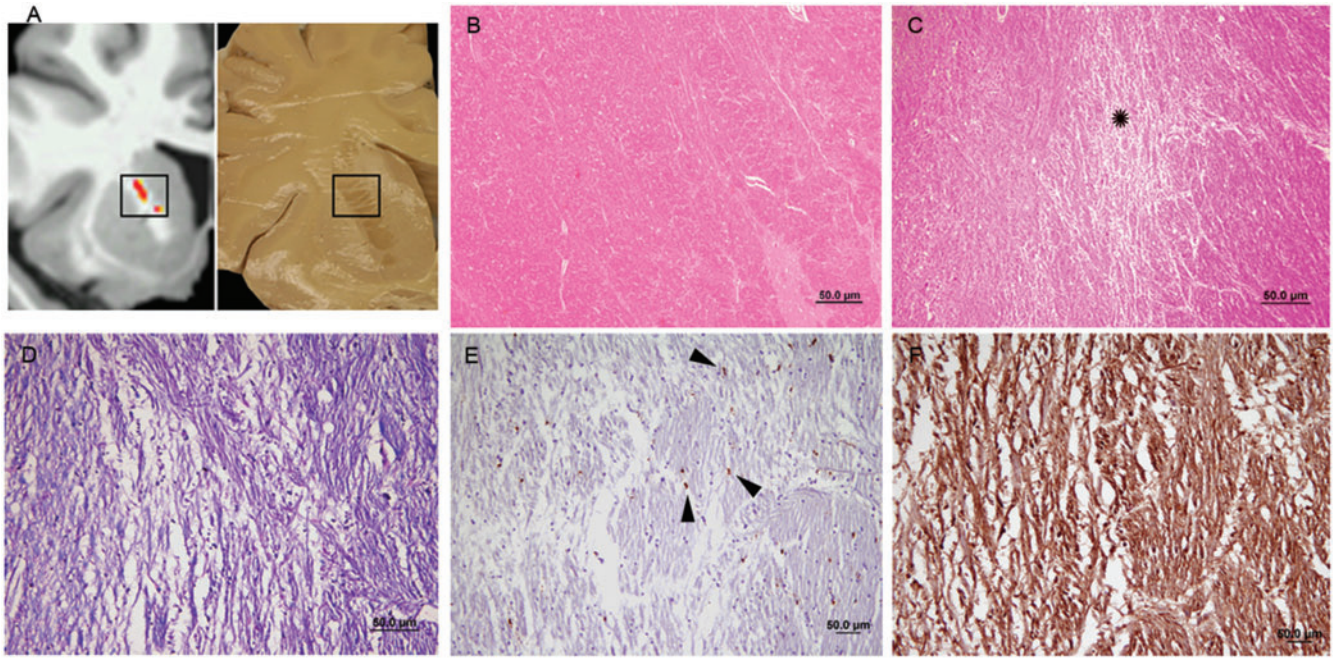

Fig. 4 DTI-guided postmortem neuropathological examination of FA changes in the genu of the internal capsule. (**A**) An example of T_1-weighted image in coronal plane with overlaid FA group differences (*left*) and visually matched *postmortem* coronal brain slice (*right*). The black box indicates the region of tissue extraction from the *postmortem* specimen. (**B**) Photomicrograph of the control sample shows well-organized white matter in the genu of the internal capsule (GIC) and (**C**) reduced white matter density (*) in the GIC in an SD patient (H&E stain). Area of reduced white matter density in the GIC reveals (**D**) reduction of myelin content (LFB/PAS stain), (**E**) diffusely scattered reactive microglial/macrophage cells (KPI stain) and (**F**) moderate reduction of axonal density (anti-NFTP stain).

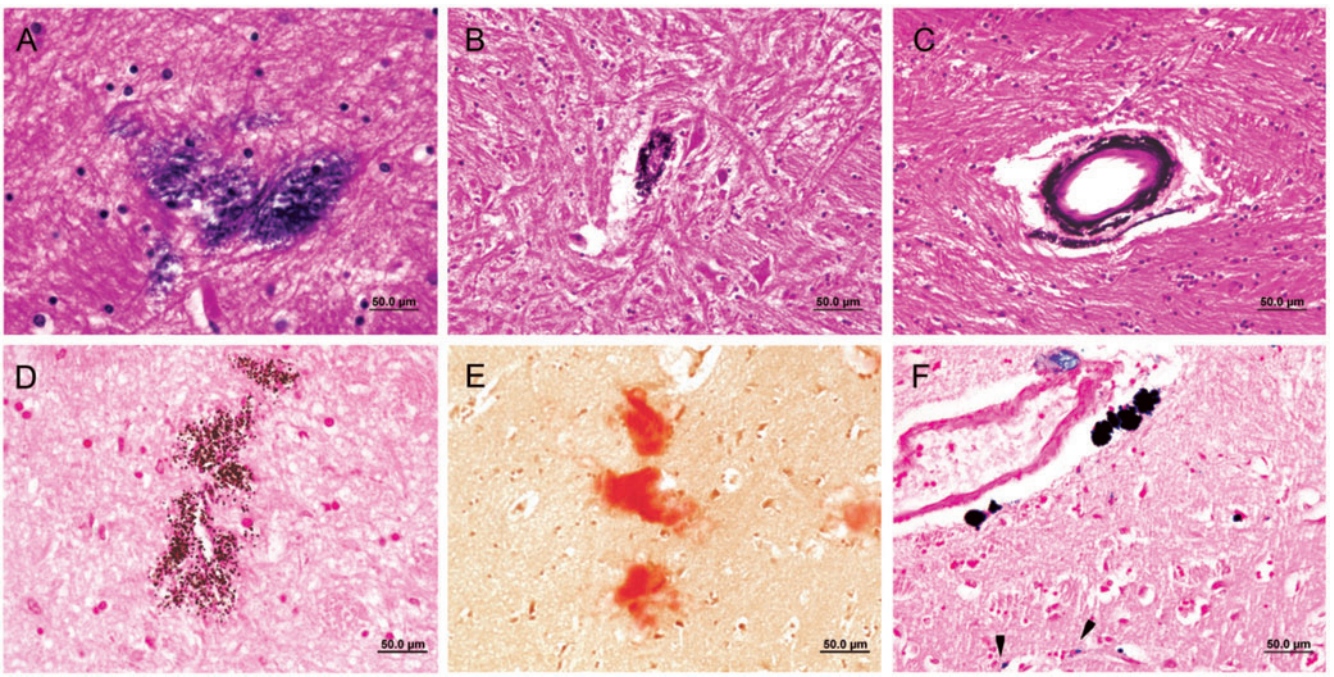

Fig. 5 DTI-guided postmortem neuropathological examination of Trace (*D*) changes in an SD patient. Photomicrographs of the mineral depositions (dark-blue/black visualization product) in the parenchyma of the putamen (**A**) and globus pallidus (**B**) and in the vessel wall in the posterior limb of the internal capsule (**C**) (H&E stain). An example from putaminal tissue shows accumulations of phosphorus (von Kossa stain) (**D**) and calcium (alizarin red S stain) (**E**) in the parenchyma and deposition of iron in the vessel wall (Prussian blue stain) (**F**) with scattered single iron-positive cells in the parenchyma (arrowheads).

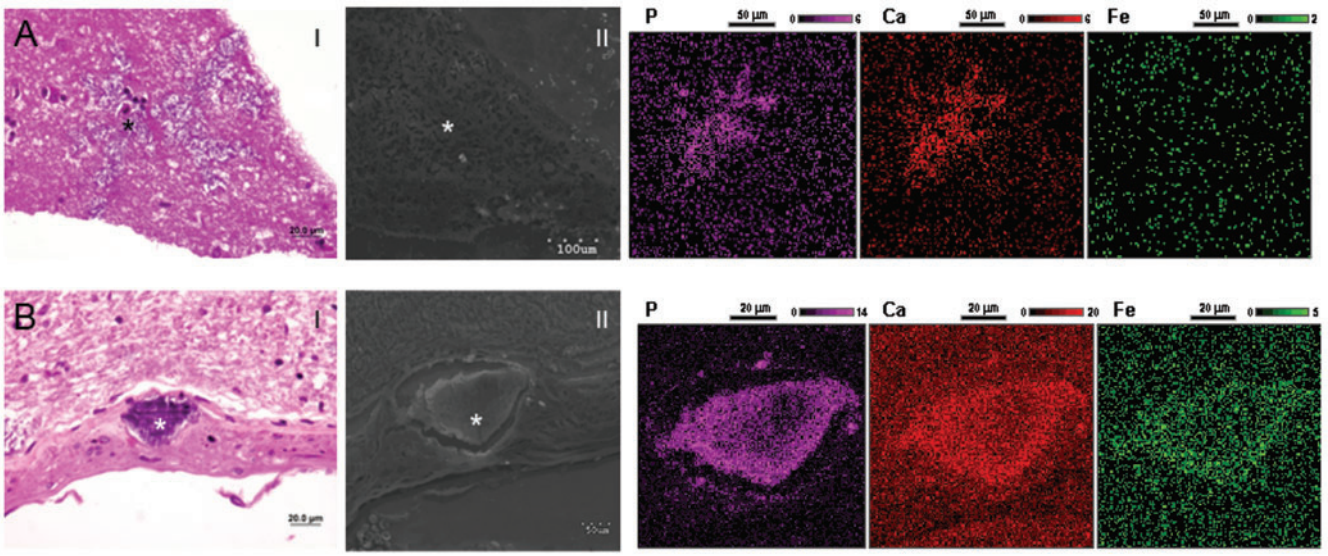

Fig. 6 Scanning electron microscopy with energy dispersive X-ray analysis (SEM-EDXA) of tissue depositions in an SD patient. (**A**) Photomicrograph of the deposition (*) in the putaminal parenchyma on H&E stain (I) and SEM (II) (scale 100 μm). EDXA shows accumulation of phosphorus (P) and calcium (Ca). (**B**) Vessel wall deposition in the putamen (*) shown on H&E stain (I) and SEM (II) (scale 50 μm). EDXA detected collocation of phosphorus (P), calcium (Ca), and iron (Fe).

pyramids to subcortical structures, including the striatum, thalamus, midbrain and brainstem nuclei (Ross, 1980; Manelfe *et al*., 1981; Tredici *et al*., 1982; Davidoff, 1990). In the internal capsule, the CBT and CST fibres are organized somatotopically with the CBT of head and neck representation occupying the genu and the CST of hand and foot representation traversing the posterior third quarter of the posterior limb (Tredici *et al*., 1982; Bogousslavsky and Regli, 1990; Aoki *et al*., 2005; Holodny *et al*., 2005). Focal ischaemic lesions in the genu of the internal capsule have been reported to cause orofacial and laryngeal paresis in stroke patients due to massive disruption of the corticobulbar tract (Manelfe *et al*., 1981; Soisson *et al*., 1982; Tredici *et al*., 1982; Bogousslavsky and Regli, 1990). The microstructural abnormalities in the internal capsule in SD patients reported here are relatively subtle and confined, suggesting the presence of the different pathological process.

The most specific disorganization of CBT/CST in SD was found in the genu of the internal capsule demonstrating right-localized anisotropy decrease, bilateral diffusivity increase and white matter thinning. Although the precise neural correlates of altered anisotropy and diffusivity are not well understood, these measures are thought to be linked to the quality and density of axonal tracts in the brain (Horsfield and Jones, 2002; Le Bihan and van Zijl, 2002). This was confirmed by our *postmortem* findings in an SD patient, which demonstrated reduced axonal course and myelin content in the right genu of the internal capsule, where DTI changes were identified in a larger group of living SD patients. The observed increase in microglial activation in the region of these focal changes may suggest that axonal degeneration could be secondary to a slow demyelination process in this region. Alternatively, the loss of myelin could be secondary to a cell loss within the laryngeal motor cortex and concomitant axonal degeneration. A limitation of this study is the unavailability of the patient's *postmortem* tissue from the laryngeal/orofacial sensorimotor cortex, which rendered us unable to further examine the possible motor cortical involvement that may have been related to white matter changes in the genu of the internal capsule in SD. Detailed interpretation of these findings will require future access to the *postmortem* tissue from the laryngeal motor cortex and internal capsule of both hemispheres for stereological analyses of cortical neuron distribution and axonal density, respectively, in SD patients compared to controls.

Although the DTI study found a highly significant right-lateralized FA abnormalities in SD patients compared to controls, these results were rather unexpected in a disorder, which is task-specific to speech production, usually dominant to the left hemisphere (Binder *et al*., 1995; Desmond *et al*., 1995; Bookheimer *et al*., 1997; Price, 2000; Vernooij *et al*., 2007). However, our finding is in line with a recent fMRI study in patients with ADSD, which has reported symptom-specific functional activation changes localized to the right ventral sensorimotor region during voluntary voice production (Haslinger *et al*., 2005).

Increased diffusivity along the CBT/CST is thought to reflect changes in relative intracellular/extracellular volumes or net loss of structural barriers of diffusion due to cell loss and impaired connectivity within the white matter (Pierpaoli *et al*., 1996; Gass *et al*., 2001; Kantarci *et al*., 2001; Beaulieu, 2002; Sykova, 2004). Mineral accumulations

in the internal capsule of the SD patient found in this study may contribute to water diffusivity changes. Mineral depositions were not observed in our control brain tissue samples, therefore, these abnormalities in the patient's brain may be due to a primary neurological process or a generalized metabolic disorder associated with a disruption in the blood-brain barrier (Casanova and Araque, 2003).

DTI measures were not significantly different between the SD and HV groups in the region of cingulum underlying the anterior cingulate cortex (ACC). The ACC controls voluntary voice initiation and vocal expression of emotional states (Jurgens and von Cramon, 1982; Jurgens, 2002). Although the ACC is reciprocally connected with the laryngeal motor cortex (Simonyan and Jurgens, 2002, 2005), absence of microstructural differences in the white matter underlying the ACC demonstrates a separation of the affected voluntary vocal motor control from unaffected voluntary vocal emotional control in SD patients.

Our study points to the selective abnormalities affecting the voluntary vocal motor control pathway with the abnormalities in the genu of the internal capsule appearing as the most specific disorder-related finding in SD.

Basal ganglia and thalamus

The link between dystonia and basal ganglia dysfunction has been apparent (Berardelli *et al.*, 1998; Hallett, 1998). Basal ganglia balance excitation and inhibition of the thalamo-cortical circuit involved in motor execution. This balance is thought to be altered in task-specific dystonias due to reduced GABAergic metabolism (Levy and Hallett, 2002) and dopaminergic receptor binding (Perlmutter *et al.*, 1997), leading to excessive motor cortical excitation (Hallett, 1998). In a review of 240 cases of lesions in basal ganglia from various causes, Bhatia and Marsden found secondary dystonia to be the most common symptom, occurring in 36% of lesions (Bhatia and Marsden, 1994). Most of these small lesions were located in the lentiform nucleus, particularly in the putamen. Recent neuroimaging studies in other forms of primary dystonia have confirmed the presence of functional and structural changes in the basal ganglia (Black *et al.*, 1998; Eidelberg, 1998; Meunier *et al.*, 2003; Colosimo *et al.*, 2005; Blood *et al.*, 2006; Bonilha *et al.*, 2007).

In this study, diffusivity changes and correlated histopathological abnormalities presented as mineral accumulations of calcium, phosphorus and iron in the parenchyma and vessels of the putamen and globus pallidus were found in SD patients. Equilibrium of calcium and iron distribution is of biological importance for electron exchange and oxidation–reduction reactions. Increases in calcium and iron levels enhance lipid peroxidation and, therefore, can mediate cell membrane damage and degeneration (Casanova and Araque, 2003). Excitotoxic effect of calcium accumulation has been reported in a wide variety of neurological diseases (Casanova and Araque, 2003), including a family with autosomal dominant dystonia-plus syndrome (Wszolek *et al.*, 2006). Iron-induced oxidative processes have been shown to reduce GABAergic inhibition (Zhang *et al.*, 1989) and cause degeneration of the dopaminergic neurons (Sastry and Arendash, 1995). Mineral accumulation in the putamen and globus pallidus found here in SD, therefore, likely underlie the abnormal metabolic processes within the basal ganglia-thalamo-cortical circuitry in SD. Future studies will need to elucidate the relationship between the neurotransmitter and mineral levels in SD and other forms of dystonia. Together with common findings of neuroimaging changes in the basal ganglia and thalamus in other forms of dystonia (Black *et al.*, 1998; Carbon *et al.*, 2004; Colosimo *et al.*, 2005; Blood *et al.*, 2006; Bonilha *et al.*, 2007), our finding of specific histopathological abnormalities in SD underlines a critical involvement of these brain regions in the pathophysiology of primary dystonias (Hallett, 2004).

Cerebellum

We found increased diffusivity in the middle cerebellar peduncle and the deep cerebellar white and grey matter in the patient group, associated with mineral accumulations found in our single SD patient. The cerebellum is involved in the motor control via the ventrolateral thalamus and has a modulatory role in coordination of voice and speech production (Arbib, 1981; Wildgruber *et al.*, 2001; Guenther *et al.*, 2006). Cerebellar dysfunction (Galardi *et al.*, 1996; Ceballos-Baumann *et al.*, 1997; Eidelberg, 1998; Odergren *et al.*, 1998; Hutchinson *et al.*, 2000; Preibisch *et al.*, 2001; Ali *et al.*, 2006) and atrophy (Fletcher *et al.*, 1988; Le Ber *et al.*, 2006) have been reported in a heterogeneous group of patients with dystonia suggesting that this disorder may arise from cerebellar disorganization. This has been supported by studies in rodent models of dystonia showing that primarily cerebellar dysfunction can cause dystonia (Brown and Lorden, 1989; Campbell and Hess, 1998; Richter *et al.*, 1998; Pizoli *et al.*, 2002; Jinnah and Hess, 2006), while cerebellectomy and selective destruction of Purkinje cells can eliminate dystonic symptoms (LeDoux *et al.*, 1993; Campbell *et al.*, 1999). Microstructural abnormalities in the cerebellum and ventral thalamus found in the present study may possibly weaken the cerebello-thalamo-cortical modulatory input in SD and, therefore, play a role in the pathophysiology of dystonia.

Clinical correlations

Measures of water diffusivity were positively correlated with the clinical symptoms of SD, e.g. with the number of voice breaks in sentences. These results together with *postmortem* findings of focal abnormalities in an SD patient treated with botulinum toxin over 10 years until death suggest that microstructural changes may represent primary brain changes contributing to the pathophysiology of this disorder. Discrepancies between our results and recent

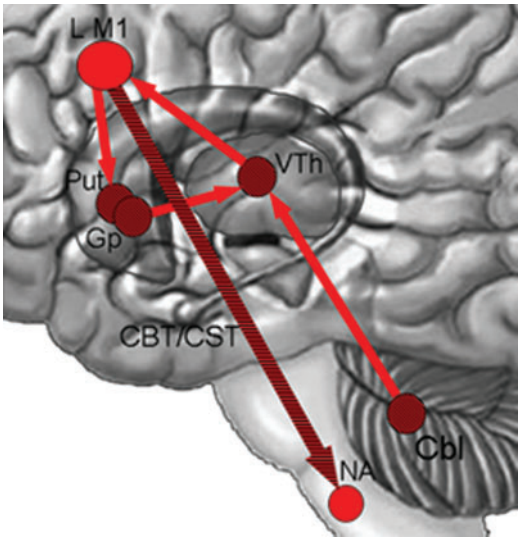

Fig. 7 Simplified schematic illustration of the neural network of voluntary laryngeal control in humans. Direct projections from the laryngeal motor cortex (LMI) to the phonatory motor nuclei (nucleus ambiguus, NA) descend via the corticobulbar/corticospinal tract (CBT/CST). Several connections exist between the LMI and the subcortical motor system. The putamen (Put) receives input from the LMI and projects back to the LMI via the globus pallidus (Gp) and ventral lateral thalamus (VTh) forming striato-pallido-thalamo-cortical loop. Cerebellar motor input (Cbl) to the LMI is via the VTh. Microstructural changes along the CBT/CST as well as in the regions directly or indirectly contributing to the CBT/CST found in this study (dashed areas) may affect voluntary laryngeal control in patients with SD.

DTI findings in four patients with cervical dystonia reporting reversal of white matter changes after botulinum toxin treatment (Blood *et al.*, 2006) may be explained by a larger sample size and more detailed evaluation of the white matter organization in the present study.

It is notable that our study included patients with adductor and abductor SD. Although symptoms of these two types of SD differ, both are characterized by the loss of the *voluntary* control of voice production. This learned behaviour in humans, involving both voluntary adductor and abductor laryngeal movements for speech production, is under control of the laryngeal motor cortex with direct input to the nucleus ambiguus and reticular formation of the brainstem via the CBT (Kuypers, 1958; Jurgens and Ehrenreich, 2007). Therefore, it is unlikely that the differential changes would be found in the white matter tracts between the patients with adductor and abductor SD.

Conclusion

The present study is among the first detailed investigations of the neuropathological basis of SD. Our findings suggest that altered microstructural integrity of the CBT/CST may represent primary neurological changes in SD. Focal microstructural changes along the CBT/CST as well as in the regions directly or indirectly contributing to the CBT/CST are likely to alter the communication between cortical and subcortical brain regions that are essential for voluntary voice control for speech production (Fig. 7). A slow progressive neurodegenerative or metabolic processes in these brain regions may underlie the abnormalities in the microstructural brain organization and, therefore, contribute to the pathophysiology of this disorder. White matter abnormalities in the genu of the internal capsule, where head and neck muscles are represented, are the most *specific* disorder-related findings in SD. On the other hand, DTI changes in the basal ganglia, thalamus and cerebellum in SD represent a common neuroimaging finding in patients with primary dystonias. We substantiated these neuroimaging findings with specific histopathological abnormalities presented as clusters of mineral accumulations in these brain regions in SD, which may contribute to a *common* neuropathological process in the focal dystonias.

Supplementary material

Supplementary material is available at *Brain* online.

Acknowledgements

We thank Drs Susumu Mori and Xin Li for software support, Drs Noriaki Hattori and S. Lalith Talagala for image acquisition support, Dr Carlo Pierpaoli for advice in data analysis, Dr Pamela R. Kearney for participants' clinical screening, Sandra B. Martin for assistance with patient recruitment and Kimberly Finnegan for rating the voice and speech samples. We are grateful to Viktoria Baker, Laboratory of Pathology, NCI, for histology preparations, and to Dr Mark Raffeld and Cynthia Harris, Molecular Pathology Section, NCI, for immunohistochemistry preparations. Tissue specimens were obtained from the NICHD Brain and Tissue Bank for Developmental Disorders at University of Maryland, Baltimore, MD and from the Human Brain and Spinal Fluid Resource Center, VAMC, Los Angeles, CA, sponsored by NINDS/NIMH, National Multiple Sclerosis Society, VA Greater Los Angeles Healthcare System and Veterans Health Services and Research Administration, Department of Veterans Affairs. This work was supported by the Intramural Program of the National Institute of Neurological Disorders and Stroke.

References

Ali SO, Thomassen M, Schulz GM, Hosey LA, Varga M, Ludlow CL, et al. Alterations in CNS activity induced by botulinum toxin treatment in spasmodic dysphonia: an H215O PET study. J Speech Lang Hear Res 2006; 49: 1127–46.

Aoki S, Iwata NK, Masutani Y, Yoshida M, Abe O, Ugawa Y, et al. Quantitative evaluation of the pyramidal tract segmented by diffusion tensor tractography: feasibility study in patients with amyotrophic lateral sclerosis. Radiat Med 2005; 23: 195–9.

Arbib M. Preceptual structures and distributed motor control. In: Brookhart JM MV, editor. Handbook of physiology. Motor control. Vol. 2. Bethesda: Americal Physiological Society; 1981. pp. 1449–80.

Barkmeier JM, Case JL, Ludlow CL. Identification of symptoms for spasmodic dysphonia and vocal tremor: a comparison of expert and nonexpert judges. J Commun Disord 2001; 34: 21–37.

Basser PJ, Mattiello J, LeBihan D. MR diffusion tensor spectroscopy and imaging. Biophys J 1994; 66: –259–67.

Beaulieu C. The basis of anisotropic water diffusion in the nervous system – a technical review. NMR Biomed 2002; 15: –435–55.

Berardelli A, Rothwell JC, Hallett M, Thompson PD, Manfredi M, Marsden CD. The pathophysiology of primary dystonia. Brain 1998; 121 (Pt 7): 1195–212.

Bhatia KP, Marsden CD. The behavioural and motor consequences of focal lesions of the basal ganglia in man. Brain 1994; 117 (Pt 4): 859–76.

Bielamowicz S, Ludlow CL. Effects of botulinum toxin on pathophysiology in spasmodic dysphonia. Ann Otol Rhinol Laryngol 2000; 109: 194–203.

Binder JR, Rao SM, Hammeke TA, Frost JA, Bandettini PA, Jesmanowicz A, et al. Lateralized human brain language systems demonstrated by task subtraction functional magnetic resonance imaging. Arch Neurol 1995; 52: 593–601.

Black KJ, Ongur D, Perlmutter JS. Putamen volume in idiopathic focal dystonia. Neurology 1998; 51: 819–24.

Bloch CS, Hirano M, Gould WJ. Symptom improvement of spastic dysphonia in response to phonatory tasks. Ann Otol Rhinol Laryngol 1985; 94: 51–4.

Blood AJ, Tuch DS, Makris N, Makhlouf ML, Sudarsky LR, Sharma N. White matter abnormalities in dystonia normalize after botulinum toxin treatment. Neuroreport 2006; 17: 1251–5.

Bogousslavsky J, Regli F. Capsular genu syndrome. Neurology 1990; 40: 1499–502.

Bonilha L, de Vries PM, Vincent DJ, Rorden C, Morgan PS, Hurd MW, et al. Structural white matter abnormalities in patients with idiopathic dystonia. Mov Disord 2007; 22: 1110–6.

Bookheimer SY, Zeffiro TA, Blaxton T, Malow BA, Gaillard WD, Sato S, et al. A direct comparison of PET activation and electrocortical stimulation mapping for language localization. Neurology 1997; 48: 1056–65.

Brown LL, Lorden JF. Regional cerebral glucose utilization reveals widespread abnormalities in the motor system of the rat mutant dystonic. J Neurosci 1989; 9: 4033–41.

Campbell DB, Hess EJ. Cerebellar circuitry is activated during convulsive episodes in the tottering (tg/tg) mutant mouse. Neuroscience 1998; 85: 773–83.

Campbell DB, North JB, Hess EJ. Tottering mouse motor dysfunction is abolished on the Purkinje cell degeneration (pcd) mutant background. Exp Neurol 1999; 160: 268–78.

Carbon M, Kingsley PB, Su S, Smith GS, Spetsieris P, Bressman S, et al. Microstructural white matter changes in carriers of the DYT1 gene mutation. Ann Neurol 2004; 56: 283–6.

Casanova MF, Araque JM. Mineralization of the basal ganglia: implications for neuropsychiatry, pathology and neuroimaging. Psychiatry Res 2003; 121: 59–87.

Ceballos-Baumann AO, Sheean G, Passingham RE, Marsden CD, Brooks DJ. Botulinum toxin does not reverse the cortical dysfunction associated with writer's cramp. A PET study. Brain 1997; 120 (Pt 4): 571–82.

Colosimo C, Pantano P, Calistri V, Totaro P, Fabbrini G, Berardelli A. Diffusion tensor imaging in primary cervical dystonia. J Neurol Neurosurg Psychiatry 2005; 76: 1591–3.

Davidoff RA. The pyramidal tract. Neurology 1990; 40: 332–9.

Desmond JE, Sum JM, Wagner AD, Demb JB, Shear PK, Glover GH, et al. Functional MRI measurement of language lateralization in Wada-tested patients. Brain 1995; 118 (Pt 6): 1411–9.

Edgar JD, Sapienza CM, Bidus K, Ludlow CL. Acoustic measures of symptoms in abductor spasmodic dysphonia. J Voice 2001; 15: 362–72.

Eidelberg D. Functional brain networks in movement disorders. Curr Opin Neurol 1998; 11: 319–26.

Fletcher NA, Stell R, Harding AE, Marsden CD. Degenerative cerebellar ataxia and focal dystonia. Mov Disord 1988; 3: 336–42.

Furutani K, Harada M, Minato M, Morita N, Nishitani H. Regional changes of fractional anisotropy with normal aging using statistical parametric mapping (SPM). J Med Invest 2005; 52: 186–90.

Galardi G, Perani D, Grassi F, Bressi S, Amadio S, Antoni M, et al. Basal ganglia and thalamo-cortical hypermetabolism in patients with spasmodic torticollis. Acta Neurol Scand 1996; 94: 172–6.

Gass A, Niendorf T, Hirsch JG. Acute and chronic changes of the apparent diffusion coefficient in neurological disorders–biophysical mechanisms and possible underlying histopathology. J Neurol Sci 2001; 186 (Suppl 1): S15–23.

Guenther FH, Ghosh SS, Tourville JA. Neural modeling and imaging of the cortical interactions underlying syllable production. Brain Lang 2006; 96: 280–301.

Hallett M. The neurophysiology of dystonia. Arch Neurol 1998; 55: 601–3.

Hallett M. Dystonia: abnormal movements result from loss of inhibition. Adv Neurol 2004; 94: 1–9.

Haslinger B, Erhard P, Dresel C, Castrop F, Roettinger M, Ceballos-Baumann AO. "Silent event-related" fMRI reveals reduced sensorimotor activation in laryngeal dystonia. Neurology 2005; 65: 1562–9.

Holodny AI, Gor DM, Watts R, Gutin PH, Ulug AM. Diffusion-tensor MR tractography of somatotopic organization of corticospinal tracts in the internal capsule: initial anatomic results in contradistinction to prior reports. Radiology 2005; 234: 649–53.

Horsfield MA, Jones DK. Applications of diffusion-weighted and diffusion tensor MRI to white matter diseases - a review. NMR Biomed 2002; 15: 570–7.

Hutchinson M, Nakamura T, Moeller JR, Antonini A, Belakhlef A, Dhawan V, et al. The metabolic topography of essential blepharospasm: a focal dystonia with general implications. Neurology 2000; 55: 673–7.

Iwatsubo T, Kuzuhara S, Kanemitsu A, Shimada H, Toyokura Y. Corticofugal projections to the motor nuclei of the brainstem and spinal cord in humans. Neurology 1990; 40: 309–12.

Jiang H, van Zijl PC, Kim J, Pearlson GD, Mori S. DtiStudio: resource program for diffusion tensor computation and fiber bundle tracking. Comput Methods Programs Biomed 2006; 81: 106–16.

Jinnah HA, Hess EJ. A new twist on the anatomy of dystonia: the basal ganglia and the cerebellum? Neurology 2006; 67: 1740–1.

Jurgens U. Neural pathways underlying vocal control. Neurosci Biobehav Rev 2002; 26: 235–58.

Jurgens U, Ehrenreich L. The descending motorcortical pathway to the laryngeal motoneurons in the squirrel monkey. Brain Res 2007; 1148: 90–5.

Jurgens U, von Cramon D. On the role of the anterior cingulate cortex in phonation: a case report. Brain Lang 1982; 15: 234–48.

Kantarci K, Jack CR Jr, Xu YC, Campeau NG, O'Brien PC, Smith GE, et al. Mild cognitive impairment and Alzheimer disease: regional diffusivity of water. Radiology 2001; 219: 101–7.

Karnell MP, Melton SD, Childes JM, Coleman TC, Dailey SA, Hoffman HT. Reliability of clinician-based (GRBAS and CAPE-V) and patient-based (V-RQOL and IPVI) documentation of voice disorders. J Voice 2007; 21: 576–90.

Kulisevsky J, Marti MJ, Ferrer I, Tolosa E. Meige syndrome: neuropathology of a case. Mov Disord 1988; 3: 170–5.

Kuypers HG. Corticobular connexions to the pons and lower brain-stem in man: an anatomical study. Brain 1958; 81: 364–88.

Le Ber I, Clot F, Vercueil L, Camuzat A, Viemont M, Benamar N, et al. Predominant dystonia with marked cerebellar atrophy: a rare phenotype in familial dystonia. Neurology 2006; 67: 1769–73.

Le Bihan D, van Zijl P. From the diffusion coefficient to the diffusion tensor. NMR Biomed 2002; 15: 431–4.

LeDoux MS, Lorden JF, Ervin JM. Cerebellectomy eliminates the motor syndrome of the genetically dystonic rat. Exp Neurol 1993; 120: 302–10.

Levy LM, Hallett M. Impaired brain GABA in focal dystonia. Ann Neurol 2002; 51: 93–101.

Ludlow CL, Schulz GM, Yamashita T, Deleyiannis FW. Abnormalities in long latency responses to superior laryngeal nerve stimulation in

adductor spasmodic dysphonia. Ann Otol Rhinol Laryngol 1995; 104: 928–35.

Manelfe C, Clanet M, Gigaud M, Bonafe A, Guiraud B, Rascol A. Internal capsule: normal anatomy and ischemic changes demonstrated by computed tomography. AJNR. Am J Neuroradiol 1981; 2: 149–55.

McNaught KS, Kapustin A, Jackson T, Jengelley TA, Jnobaptiste R, Shashidharan P, et al. Brainstem pathology in DYT1 primary torsion dystonia. Ann Neurol 2004; 56: 540–7.

Meunier S, Lehericy S, Garnero L, Vidailhet M. Dystonia: lessons from brain mapping. Neuroscientist 2003; 9: 76–81.

Mori S, Wakana, S, van Zijl PCM, Nagae-Poetscher LM. MRI atlas of human white matter. Elsevier Science; Amsterdam, The Netherlands, 2005.

Nash EA, Ludlow CL. Laryngeal muscle activity during speech breaks in adductor spasmodic dysphonia. Laryngoscope 1996; 106: 484–9.

Nichols TE, Holmes AP. Nonparametric permutation tests for functional neuroimaging: a primer with examples. Hum Brain Mapp 2002; 15: 1–25.

Odergren T, Stone-Elander S, Ingvar M. Cerebral and cerebellar activation in correlation to the action-induced dystonia in writer's cramp. Mov Disord 1998; 13: 497–508.

Pajevic S, Pierpaoli C. Color schemes to represent the orientation of anisotropic tissues from diffusion tensor data: application to white matter fiber tract mapping in the human brain. Magn Reson Med 1999; 42: 526–40.

Perlmutter JS, Stambuk MK, Markham J, Black KJ, McGee-Minnich L, Jankovic J, et al. Decreased [18F]spiperone binding in putamen in idiopathic focal dystonia. J Neurosci 1997; 17: 843–50.

Pfefferbaum A, Sullivan EV. Increased brain white matter diffusivity in normal adult aging: relationship to anisotropy and partial voluming. Magn Reson Med 2003; 49: 953–61.

Pierpaoli C, Barnett A, Pajevic S, Chen R, Penix LR, Virta A, et al. Water diffusion changes in Wallerian degeneration and their dependence on white matter architecture. Neuroimage 2001; 13: 1174–85.

Pierpaoli C, Jezzard P, Basser PJ, Barnett A, Di Chiro G. Diffusion tensor MR imaging of the human brain. Radiology 1996; 201: 637–48.

Pizoli CE, Jinnah HA, Billingsley ML, Hess EJ. Abnormal cerebellar signaling induces dystonia in mice. J Neurosci 2002; 22: 7825–33.

Preibisch C, Berg D, Hofmann E, Solymosi L, Naumann M. Cerebral activation patterns in patients with writer's cramp: a functional magnetic resonance imaging study. J Neurol 2001; 248: 10–7.

Price CJ. The anatomy of language: contributions from functional neuroimaging. J Anat 2000; 197 (Pt 3): 335–59.

Richter A, Brotchie JM, Crossman AR, Loscher W. [3H]-2-deoxyglucose uptake study in mutant dystonic hamsters: abnormalities in discrete brain regions of the motor system. Mov Disord 1998; 13: 718–25.

Ross ED. Localization of the pyramidal tract in the internal capsule by whole brain dissection. Neurology 1980; 30: 59–64.

Rueckert D, Sonoda LI, Hayes C, Hill DL, Leach MO, Hawkes DJ. Nonrigid registration using free-form deformations: application to breast MR images. IEEE. Trans Med Imaging 1999; 18: 712–21.

Sapienza CM, Walton S, Murry T. Adductor spasmodic dysphonia and muscular tension dysphonia: acoustic analysis of sustained phonation and reading. J Voice 2000; 14: 502–20.

Sastry S, Arendash GW. Time-dependent changes in iron levels and associated neuronal loss within the substantia nigra following lesions within the neostriatum/globus pallidus complex. Neuroscience 1995; 67: 649–66.

Simonyan K, Jurgens U. Cortico-cortical projections of the motorcortical larynx area in the rhesus monkey. Brain Res 2002; 949: 23–31.

Simonyan K, Jurgens U. Afferent cortical connections of the motor cortical larynx area in the rhesus monkey. Neuroscience 2005; 130: 133–49.

Smith SM. Fast robust automated brain extraction. Hum Brain Mapp 2002; 17: 143–55.

Smith SM, Jenkinson M, Johansen-Berg H, Rueckert D, Nichols TE, Mackay CE, et al. Tract-based spatial statistics: voxelwise analysis of multi-subject diffusion data. Neuroimage 2006; 31: 1487–505.

Soisson T, Cabanis EA, Iba-Zizen MT, Bousser MG, Laplane D, Castaigne P. Pure motor hemiplegia and computed tomography. 19 cases. J Neuroradiol 1982; 9: 304–22.

Sykova E. Extrasynaptic volume transmission and diffusion parameters of the extracellular space. Neuroscience 2004; 129: 861–76.

Tredici G, Pizzini G, Bogliun G, Tagliabue M. The site of motor corticospinal fibres in the internal capsule of man. A computerised tomographic study of restricted lesions. J Anat 1982; 134: 199–208.

Vernooij MW, Smits M, Wielopolski PA, Houston GC, Krestin GP, van der Lugt A. Fiber density asymmetry of the arcuate fasciculus in relation to functional hemispheric language lateralization in both right- and left-handed healthy subjects: a combined fMRI and DTI study. Neuroimage 2007; 35: 1064–76.

Wildgruber D, Ackermann H, Grodd W. Differential contributions of motor cortex, basal ganglia, and cerebellum to speech motor control: effects of syllable repetition rate evaluated by fMRI. Neuroimage 2001; 13: 101–9.

Woods RP, Grafton ST, Holmes CJ, Cherry SR, Mazziotta JC. Automated image registration: I. General methods and intrasubject, intramodality validation. J Comput Assist Tomogr 1998; 22: 139–52.

Wszolek ZK, Baba Y, Mackenzie IR, Uitti RJ, Strongosky AJ, Broderick DF, et al. Autosomal dominant dystonia-plus with cerebral calcifications. Neurology 2006; 67: 620–5.

Zhang ZH, Zuo QH, Wu XR. Effects of lipid peroxidation on GABA uptake and release in iron-induced seizures. Chin Med J 1989; 102: 24–7.

Zweig RM, Hedreen JC. Brain stem pathology in cranial dystonia. Adv Neurol 1988; 49: 395–407.